

# Selective growth of silica nanowires on nickel nanostructures created by atomic force microscopy nanomachining

Ju-Hung Hsu, Ming-Hung Huang, Hsiao-Hsien Lin and Heh-Nan Lin<sup>1</sup>

Department of Materials Science and Engineering, National Tsing Hua University, Hsinchu 300, Taiwan

E-mail: [hnlin@mx.nthu.edu.tw](mailto:hnlin@mx.nthu.edu.tw)

Received 14 September 2005, in final form 25 October 2005

Published 1 December 2005

Online at [stacks.iop.org/Nano/17/170](http://stacks.iop.org/Nano/17/170)

## Abstract

We report the selective growth of amorphous silica nanowires on nickel nanostructures created by an atomic force microscopy nanomachining and lift-off process. Successful growth of patterned nanowire bunches or single nanowires on Si substrates has been realized by thermal annealing. The growth mechanism is found to be a combination of vapour–liquid–solid and solid–liquid–solid modes. In addition, the relationship between the nanowire length and the growth time has a nonlinear dependence.

(Some figures in this article are in colour only in the electronic version)

## 1. Introduction

One-dimensional nanomaterials have been the focus of extensive research activities in recent years due to their novel properties and applications in nanodevices [1]. In particular, silica nanowires have been found to emit strong blue light [2] and they can be potentially used as emitters or interconnects [3] in nanophotonic devices. For the synthesis, catalytic growth is commonly employed, and several methods, including laser ablation [2], thermal evaporation [4, 5], thermal annealing [6–8], and chemical vapour deposition [9, 10], have been reported in the literature. Two types of growth mechanism, namely vapour–liquid–solid (VLS) [1, 2, 7] and solid–liquid–solid (SLS) [6, 8, 11], have been used to explain the catalytic growth. Additionally, size control has also been realized by sol–gel methods with the use of anodic alumina membranes [12, 13].

In many applications, selective area growth of nanowires is of great importance for device construction. Taking carbon nanotubes for example, various techniques have already been utilized, such as photolithography, e-beam lithography, micro-contact printing, and shadow masking [14, 15]. Among these techniques, e-beam lithography is frequently applied to generate nanoscale catalytic templates for patterned growth

of individual nanowires. On the other hand, scanning probe lithography is well known for the effective creation of nanostructures [16], and naturally can be utilized for the selective growth of nanowires.

Since reports on the selective growth of silica nanowires have been absent in the literature to our knowledge, it would be of great interest to realize such a goal. In this paper, we report the selective growth of amorphous silica nanowires on nickel catalytic templates that are created by an atomic force microscopy (AFM) nanomachining and lift-off process [17]. Successful growth of patterned nanowire bunches or single nanowires on Si substrates has been realized by thermal annealing. In addition, the growth mechanism has also been explored.

## 2. Experiment

A schematic diagram of the experimental procedure is shown in figure 1. A solution of 1.25 wt% poly(methylmethacrylate) (PMMA) in chlorobenzene was spin-coated on a silicon substrate. After a 30 min soft baking at 150 °C, a PMMA film with a thickness of around 30 nm was produced. A commercial AFM (Smena-B, NT-MDT, Russia) and rectangular silicon probes (NSC15, MikroMasch, Russia) were employed for the experiment. By scratching or indenting the PMMA film at

<sup>1</sup> Author to whom any correspondence should be addressed.

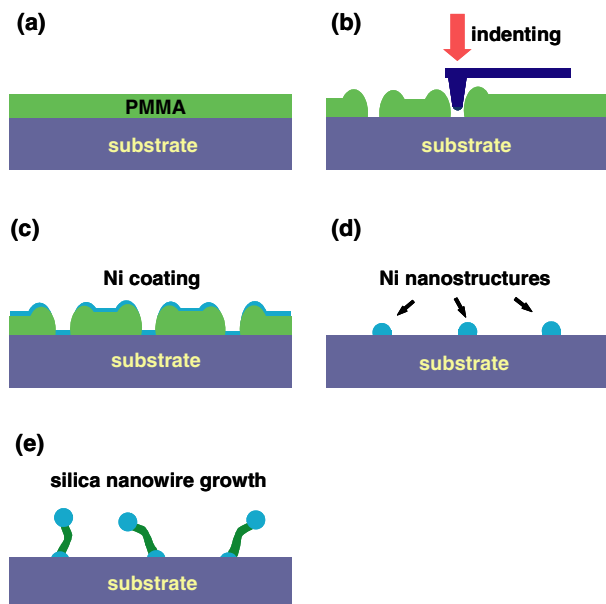


**Figure 1.** Schematic diagram of the experimental procedure. (a) A PMMA film was spin-coated on the substrate. (b) The PMMA film was scratched or indented by an AFM tip. (c) A nickel film was coated. (d) Nickel nanostructures were created after lift-off. (e) Selective growth of silica nanowires was realized by thermal annealing.

a force of  $2.2 \mu\text{N}$  with the AFM tip [17], nanopatterns were created on the film. After coating a 7 nm-thick nickel film by electron beam evaporation and soaking the sample in acetone to remove the PMMA, nickel nanostructures were successfully fabricated. Details of the AFM nanomachining procedure can be found in a previous report [17].

For the growth of silica nanowires, the sample was put in a rapid thermal annealing chamber (Mila 3000, ULVAC, Japan). A gas with a mixture of 3%  $\text{H}_2$  and 97% Ar was introduced into the chamber at a constant flow speed of 200 sccm. The vacuum inside the chamber was maintained at 200 Torr. The substrate was heated up at a rate of  $2.6^\circ\text{C s}^{-1}$  to  $1100^\circ\text{C}$ , and maintained at the temperature for a desired period of time. Morphological and structural properties were analysed by scanning electron microscopy (SEM) (JSM 6500F, JEOL, Japan) and transmission electron microscopy (TEM) (JEM 2010, JEOL, Japan).

### 3. Results and discussion

To verify if silica nanowires were grown successfully, a nickel film was first used as the catalyst. An SEM image of the result after a growth time of 20 min is shown in figure 2(a) and it clearly exhibits the generation of nanowires. A TEM image of the nanowires is shown in figure 2(b) and indicates that the diameters range roughly between 15 and 30 nm. From the electron beam diffraction pattern shown in the inset, the amorphous nature of the nanowires is ascertained. In addition, an average composition of  $\text{SiO}_{1.6}$  is determined from energy dispersive x-ray (EDX) spectrometry analysis on several nanowires. Also, the catalysts at the nanowire ends are found to be nickel silicide, as expected in consideration of the

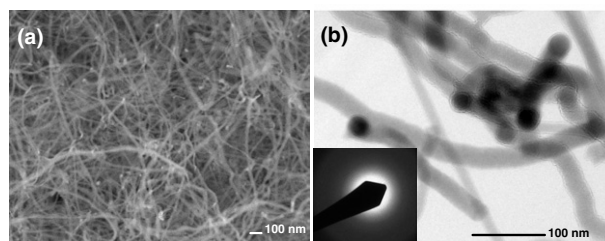


**Figure 2.** (a) SEM and (b) TEM images of silica nanowires grown at  $1100^\circ\text{C}$  for 20 min on a nickel film. The inset in (b) is the electron beam diffraction pattern.

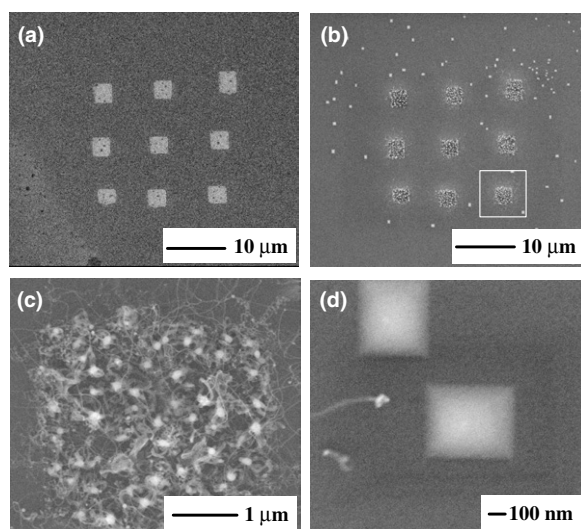


**Figure 3.** SEM images of (a) a  $3 \times 3$  array of nickel squares created by scratching, (b) the corresponding silica nanowires after a growth time of 390 s, (c) a zoomed view of the marked region in (b), and (d) a zoomed view of the scattered white spots in (b).

high growth temperature. The photoluminescence spectrum obtained with excitation from a 325 nm He–Cd laser manifests two emission peaks at 420 and 470 nm, which are in agreement with those reported in the literature [2]. All the above results confirm the successful growth of amorphous silica nanowires.

For the selective growth of silica nanowires, nickel nanostructures were created and used for subsequent catalytic growth. The SEM images of a  $3 \times 3$  array of squares created by scratching and the corresponding nanowire bunches after a growth time of 390 s are shown in figures 3(a) and (b), respectively. A zoomed image of a nanowire bunch is also shown in figure 3(c). It is interesting that there are scattered white spots outside of the original squares, as can be seen in figure 3(b). A zoomed image of the spots is provided in figure 3(d) and it reveals that there are no nanowires on these spots. An EDX analysis indicates that the major composition is nickel. It is obvious that the spots originate from the diffusion of nickel into the substrate and the subsequent transformation into nickel silicide at the high growth temperature. The spots have the shape of an inverted pyramid due to the (001) substrate plane and appear as rectangles, as in figure 3(d).

In addition to large patterns, nanodot arrays were also created by tip indenting. The AFM image of a  $10 \times 10$

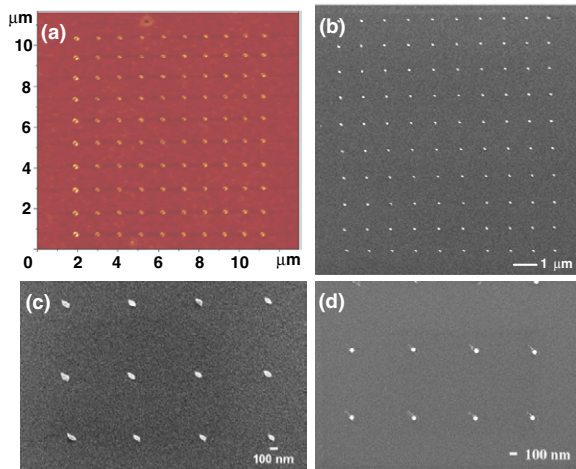


**Figure 4.** (a) AFM image of a  $10 \times 10$  nanohole array on a PMMA film created by indenting, and (b) the corresponding SEM image of the created nickel nanodots after lift-off. Zoomed SEM images of the nanodots (c) before and (d) after thermal annealing at  $1000^\circ\text{C}$  for 20 min.

nanohole array with a spacing of  $1\ \mu\text{m}$  on a PMMA film is shown in figure 4(a). The corresponding SEM image of the nickel nanodot array after lift-off is shown in figure 4(b). A zoomed image is also provided in figure 4(c) and indicates that the dot size is around 100 nm. Although the dot shape is slightly irregular, it is bound to change due to the high growth temperature. To exemplify this consequence, the SEM image of the nanodots after being annealed at  $1000^\circ\text{C}$  for 20 min is shown in figure 4(d). It is clear that the nanodots become spherical and the size has also been reduced to 60 nm.

The created nanodot arrays were then used for the selective growth of single silica nanowires. The SEM images of the results for growth periods of 300, 360, 390 and 420 s are shown in figures 5(a)–(d), respectively. The zoomed images of the marked regions in the figures are also shown in figures 5(e)–(h),

respectively. As can be seen clearly, each nanodot corresponds to a single silica nanowire. The single nanowires have a rather consistent diameter of 20 nm, which is unlike the result of a more diverse diameter range for the nanowires grown in a large area such as those shown in figure 2(a). This consequence is apparently due to the employment of nanodot catalysts with a uniform size and suggests that the present approach can be used as an effective method for size control.

From the images in figure 5, it is also obvious the each nanodot splits into two catalysts at the beginning of the nanowire growth (see figure 5(e)) and they are present at both ends of each nanowire. Furthermore, there are voids at the bottom of each nanowire, as can be clearly seen in figures 5(g) and (f). For the VLS growth mode, the catalysts are present at the nanowire tops [1, 2, 7]. For the SLS mode, the catalysts are at the nanowire roots, and the substrate becomes pitted due to diffusion of silicon [6, 8, 11]. Therefore, the present growth is apparently a combination of VLS and SLS modes. Such a consequence has not been reported previously and the origin is not clear at present time.

The nanowire length as a function of growth time can also be obtained from figure 5. However, an accurate determination of the lengths is difficult since the nanowires are highly entangled. Consequently, a straight nanowire for each growth time is chosen and used for an estimate. The chosen nanowires are marked by arrows in figures 5(e), (f), (c) and (h) and the lengths are 157, 235, 1200 and 2200 nm. The length as a function of growth time is plotted in figure 6, and a nonlinear feature is clearly seen. By fitting the data points with an exponential function, the result is

$$\ell = 0.0356 \times \exp\left(\frac{t}{38.02}\right)$$

where  $\ell$  is the length in nanometres and  $t$  the growth time in seconds. It should be noted that the exponential fit is just a convenient one but without good reasonable arguments. Nevertheless, studies of nanowire growth length as a function of time are rarely reported in the literature and the present result

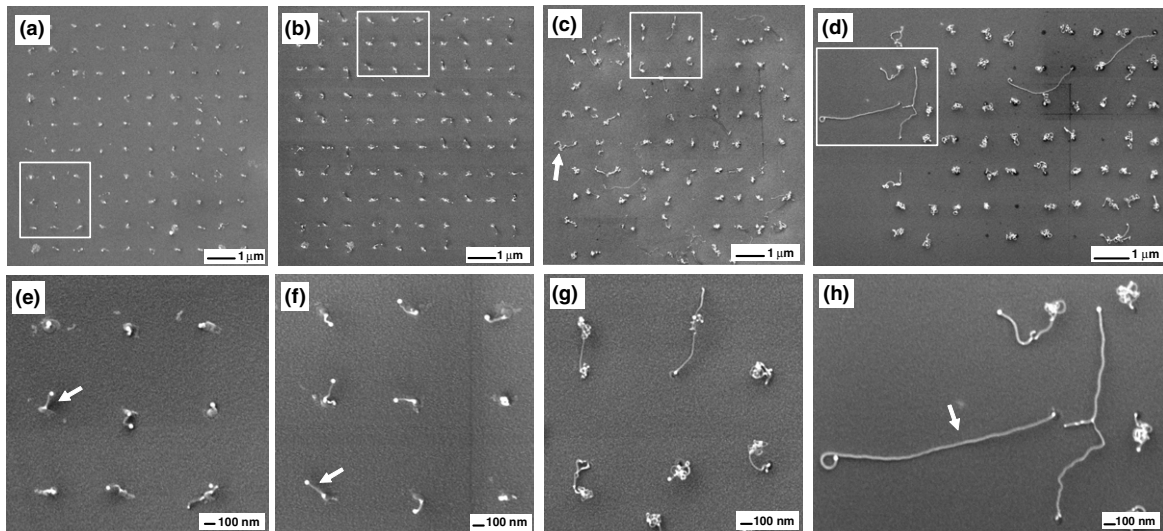


**Figure 5.** (a)–(d) SEM images of single silica nanowires grown at  $1100^\circ\text{C}$  for periods of 300, 360, 390 and 420 s, respectively, and (e)–(h) the corresponding zoomed images of the nanowires.

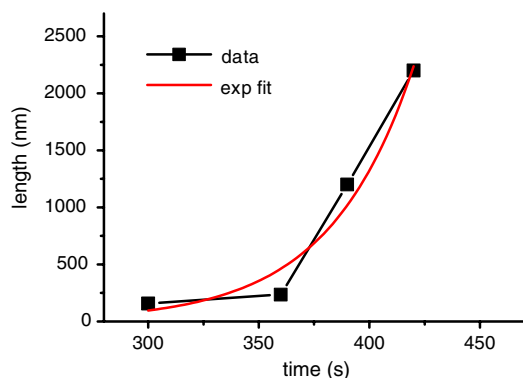


**Figure 6.** A plot of the nanowire length versus the growth time. An exponential fit is also provided.

is still of value. An investigation of the growth kinetics detail is currently under way.

#### 4. Conclusion

The selective growth of amorphous silica nanowires on nickel nanostructures by thermally annealing silicon substrates has been successfully performed. The nickel nanostructures, including squares and nanodots, are created by an AFM nanomachining and lift-off process. With the use of nickel nanodots as catalysts, single silica nanowires with a uniform diameter of 20 nm have been grown successfully. Furthermore, it is found that each nanodot catalyst splits into two nanodots and they are present at both ends of a nanowire. Consequently, the growth mechanism is considered a combination of VLS and SLS modes in contrast to reports in the literature. In addition, the nanowire length can be controlled by the growth time, and a nonlinear dependence has been observed.

#### Acknowledgments

This work was supported by the National Science Council under Grant No. 93-2216-E-007-039 and the Ministry of Education, Program for Promoting Academic Excellence under Grant No. 91-E-FA04-1-4.

#### References

- [1] Xia Y, Yang P, Sun Y, Wu Y, Mayers B, Gates B, Yin Y, Kim F and Yan H 2003 *Adv. Mater.* **15** 353–89
- [2] Yu D P, Hang Q L, Ding Y, Zhang H Z, Bai Z G, Wang J J, Zou Y H, Qian W, Xiong G C and Feng S Q 1998 *Appl. Phys. Lett.* **73** 3076–8
- [3] Tong L, Lou J, Gattass R R, He S, Chen X, Liu L and Mazur E 2005 *Nano Lett.* **5** 259–62
- [4] Liang C H, Zhang L D, Meng G W, Wang Y W and Chu Z Q 2000 *J. Non-Cryst. Solids* **277** 63–7
- [5] Chen Y J, Li J B and Dai J H 2001 *Chem. Phys. Lett.* **344** 450–6
- [6] Paulose M, Varghese O K and Grimes C A 2003 *J. Nanosci. Nanotechnol.* **3** 341–6
- [7] Elechiguerra J L, Manriquez J A and Yacaman M J 2004 *Appl. Phys. A* **79** 461–7
- [8] Park B T and Yong K 2004 *Nanotechnology* **15** S365–70
- [9] Liu Z Q, Xie S S, Sun L F, Tang D S, Zhou W Y, Wang C Y, Liu W, Li Y B, Zou X P and Wang G 2001 *J. Mater. Res.* **16** 683–6
- [10] Pan Z W, Dai Z R, Ma C and Wang Z L 2002 *J. Am. Chem. Soc.* **124** 1817–22
- [11] Yan H F, Xing Y J, Hang Q L, Yu D P, Wang Y P, Xu J, Xi Z H and Feng S Q 2000 *Chem. Phys. Lett.* **323** 224–8
- [12] Yang Z, Niu Z, Cao X, Yang Z, Lu Y, Hu Z and Han C C 2003 *Angew. Chem. Int. Edn* **42** 4201–3
- [13] Yao B, Fleming D, Morris M A and Lawrence S E 2004 *Chem. Mater.* **16** 4851–5
- [14] Dai H 2002 *Surf. Sci.* **500** 218–41
- [15] Dai L, Patil A, Gong X, Guo Z, Liu L, Liu Y and Zhu D 2003 *Chem. Phys. Chem.* **4** 1150–69
- [16] Wouters D and Schubert U S 2004 *Angew. Chem. Int. Edn* **43** 2480–95
- [17] Hsu J-H, Lin C-Y and Lin H-N 2004 *J. Vac. Sci. Technol. B* **22** 2768–71